

## Enhancing the CO<sub>2</sub> capture efficiency of amines by microgel particles

Yang Yang <sup>a,\*,\*\*</sup>, Xingguang Xu <sup>b</sup>, Yunfei Guo <sup>a</sup>, Colin D. Wood <sup>b,c,\*</sup>

<sup>a</sup> College of Energy, Chengdu University of Technology, Chengdu, 610059, People's Republic of China

<sup>b</sup> CSIRO, Energy, Australian Resources Research Centre, Kensington, 6151, Western Australia, Australia

<sup>c</sup> Curtin University of Science and Technology, Curtin Oil and Gas Innovation Centre (COGIC), Australian Resources Research Centre, Kensington, 6151, Western Australia, Australia



### ARTICLE INFO

#### Keywords:

Liquid amines

CO<sub>2</sub> capture

Sorbents

### ABSTRACT

This proof-of-concept study demonstrates a promising approach to enhance the CO<sub>2</sub> capture capacity of liquid amines, in which the amines were infused into microgel particles. A diverse range of amine infused microgels (AIMGs) were readily prepared within 5 min by adding microgel particles into different amine solutions. The AIMGs absorb CO<sub>2</sub> based on the infused amines. Due to the solid particle structure, the space among the AIMG particles provided diffusion channels for the CO<sub>2</sub> molecule and enhanced the contact efficiency of the amines and CO<sub>2</sub>. As a result, the absorption efficiency of the amines was significantly increased resulting in higher CO<sub>2</sub> uptake and faster absorption kinetics for the AIMGs compared to the conventional bulk amine solutions. Furthermore, by 'locking' the amine solutions in the microgel particles, the corrosion and foaming issues of amine solutions could be substantially mitigated. Therefore, the amine solutions which have higher concentrations than the commercial counterparts could be used in the preparation of AIMGs. Due to the thermally stable network structure, the AIMGs which were prepared by the amines with low volatility exhibited favorable cyclic capacity during the temperature-swing regeneration process.

### 1. Introduction

The ever increasing consumption of fossil fuels has resulted in the increase in the concentration of atmospheric CO<sub>2</sub>, from 270 ppm before the industrial revolution to more than 400 ppm today. It is widely believed that anthropogenic CO<sub>2</sub> is the major contributor to global climate change. Carbon capture and storage (CCS) technologies are a promising route to reduce atmospheric CO<sub>2</sub> concentration and prevent global warming. To date, the so-called "amine scrubbing" using solution of amines such as monoethanolamine (MEA), diethanolamine (DEA) and methyldiethanolamine (MDEA) are the most commercially mature and well-established technologies for CO<sub>2</sub> capture (Fine et al., 2014; Rochelle, 2009; Romeo et al., 2008). Due to the strong chemical interaction between the basic amino groups and the acidic CO<sub>2</sub> molecules, amine scrubbing is well-suited to the large-scale capture of CO<sub>2</sub> from dilute, low pressure streams. However, amine scrubbing suffers from multiple drawbacks such as corrosion, high energy consumption, evaporation loss and foaming issues (Goeppert et al., 2010; Soosaiprasadam and Veawab, 2008; Raynal et al., 2011; Yang et al., 2014). Therefore, the development of new absorbents and techniques for CO<sub>2</sub>

capture has increased in recent years.

Capturing CO<sub>2</sub> with solid adsorbents is considered as a promising alternative as the drawbacks of amine scrubbing could be overcome. The majority of solid absorbents are mesoporous and microporous materials such as porous zeolites, activated carbon, metal-organic frameworks, and microporous organic polymers (Samanta et al., 2011; Stuckert and Yang, 2011; Sumida et al., 2011; Dawson et al., 2013). The porous structure endows these absorbents with favorable CO<sub>2</sub> capture capacity based on physical adsorption. Nevertheless, the features of physical adsorption also result in some inherent drawbacks for these absorbents such as unfavorable selectivity and poor tolerance to water. The complex synthesis of these absorbents also makes large-scale production challenging. However, there has been recent progress in this space, for example, hypercrosslinked polymers have been shown to be able to absorb CO<sub>2</sub> even in the presence of water and these materials are scalable (Woodward et al., 2014).

More recently, an alkaline dry water system used for CO<sub>2</sub> capture was proposed (Dawson et al., 2014). By mixing either the neat liquid amine or the aqueous solution of inorganic alkali with silica nanoparticles at extremely high speed, the alkaline dry water absorbents

\* Corresponding author at: CSIRO, Energy, Australian Resources Research Centre, Kensington, 6151, Western Australia, Australia.

\*\* Corresponding author.

E-mail addresses: [yangyang19@cdut.edu.cn](mailto:yangyang19@cdut.edu.cn) (Y. Yang), [Colin.Wood@csiro.au](mailto:Colin.Wood@csiro.au) (C.D. Wood).

could be formed in a solid powder state. The increased contact surface area between the amines/alkali and the gas substantially enhanced the CO<sub>2</sub> absorption efficiency of the amines/alkali, which resulted in exceptional CO<sub>2</sub> capture capacity for the dry water absorbents. However, the poor recyclability and low stability of the dry water absorbents limit their application in an industrial process. We have recently reported alternative approaches using hydrogels as carriers for the amines which have demonstrated significant improvements over existing liquids (Xu et al., 2018; Xu and Wood, 2018; Xu et al., 2019). The amine infused hydrogels (AIHs) exhibited favorable CO<sub>2</sub> absorption capacity and recyclability. Nevertheless, the AIHs have relatively low surface area due to the millimeter scaled particle size and nonporous structure, which limits the further improvement in the CO<sub>2</sub> absorption capacity (efficiency).

Microgels are crosslinked polymer latex particles with sizes ranging from nanometer scale to micrometer scale. Due to the three-dimensional network and polar groups, microgels are capable of absorbing and retaining a significant amount of liquid within the network structures. In recent years, microgels have received growing attention for applications in a wide variety of areas including drug delivery, water purification, encapsulation, biomaterials, molecular imprinting, chemical sensing, catalysis, surface coatings, and emulsification (Oh et al., 2008; Nur et al., 2009; Wulff et al., 2006; Luo et al., 2010; Lu et al., 2009; Schmidt et al., 2008; Wiese et al., 2013). Microgels have also been studied in CO<sub>2</sub> capture. (Yue et al. (2014)) prepared a microgel film as a CO<sub>2</sub> absorbent which exhibited a high capacity of approximately 1.7 mmol/g in wet environment. Recently, (Yao et al. (2019)) reported a functional microgel-based hybrid nanofluid used for CO<sub>2</sub> capture. The nanofluid showed excellent stability and recycling performance. However, microgels have not been explored as micro-reactors for amines and CO<sub>2</sub>. As shown in Fig. 1, after infusing liquid amines into the molecular networks of microgel, microgel particles function as micro-reactors for amines and CO<sub>2</sub> and the liquid amines are transformed into 'solid state'. Compared to the AIHs in our previous study (Xu et al., 2018; Xu and Wood, 2018; Xu et al., 2019), the amine infused microgels (AIMGs) have smaller particle size, which endows the material with higher surface area-to-volume ratio. However, the chemical structure and CO<sub>2</sub> absorption capacity of the AIMGs are not clear. Furthermore, the mechanism of the interaction between the CO<sub>2</sub> gas and the AIMGs also requires to be comprehensively studied.

In this paper, several AIMGs were readily prepared by swelling microgels in different amine solutions. The CO<sub>2</sub> uptake, absorption kinetics, and regeneration performance of the AIMGs were comprehensively studied and compared to those of conventional bulk amine solutions. The mechanism of the interaction between the CO<sub>2</sub> gas and AIMGs were studied through the Fourier transform infrared spectroscopy (FTIR) spectra of the AIMGs before and after CO<sub>2</sub> absorption. Multiple cycles of CO<sub>2</sub> absorption and desorption were carried out to study the regeneration performance of the AIMGs.

## 2. Materials and methods

### 2.1. Materials

Acrylamide (AM, purity 99.0 %), ethanol, sodium hydroxide (NaOH, purity 97 %), polyoxyethylene sorbitan monooleate (Tween80, purity 98.0 %), sorbitan monooleate (Span80, purity 98.0 %), 2,2'-azobis(2-methylpropionamide) dihydrochloride (V-50, purity 99.0 %), and N,N'-methylene bisacrylamide (MBA, purity 99.0 %), 2-acryloylamino-2-methyl-1-propanesulfonic acid (AMPS, purity 98.0 %) were purchased from Kelong Chemical Co. (Chengdu, China). White oil was purchased from Disi Oil Co. (Chengdu, China). MEA (purity 99.5 %), DEA (purity 99.0 %), MDEA (purity 99.0 %), 2-amino-2-methyl-1-propanol (AMP, purity 99.0 %), polyethylenimine (PEI, average Mw ~ 800, purity 99.0 %) were obtained from Aldrich-sigma. All the chemicals were used as received.

### 2.2. Microgel synthesis

The microgel sample used in this study was prepared via inverse emulsion polymerization (Pu et al., 2018). The aqueous phase was a mixture of AM (11.2 g), AMPS (4.8 g), MBA (0.048 g), Tween80 (1 g) and deionized water (24 g), whereas the oil phase was comprised of Span80 (7 g) and white oil (60 g). The inverse emulsion was obtained by mixing the aqueous phase and the oil phase in a three-neck flask at room temperature using a mechanical stirrer (900) rpm for 30 min. The system was deoxygenated with nitrogen for 30 min, and then polymerization was initiated by using 0.02 g of V-50 at 50 °C under 300 rpm stirring. After 3 h, the microgel sample was isolated from the mixture via precipitating, filtering, and was subsequently washed with ethanol to remove the remaining chemicals. Afterwards, the dry microgel sample was obtained after being dried in a vacuum oven at 40 °C for 48 h. It is worth noting that AM and AMPS were chosen as the monomers for the synthesis of the microgel, which is different from the conventional super absorbent hydrogel comprising of AM and Sodium Acrylate (or Potassium Acrylate). This is because the AMPS can enhance the thermal stability of the macromolecular chain (Zhu et al., 2018). The large pendant group of the AMPS could also improve the rigidity of the macromolecular network structure, which endows the microgel with better recyclability during the temperature-swing regeneration process.

### 2.3. Characterization of the microgel and the AIMGs

The Fourier transform infrared spectroscopy (FTIR) spectra of different samples were obtained with a Tensor II Fourier transform infrared spectrophotometer (Bruker, Germany) using a diamond ATR accessory and a room temperature DLaTGS detector. Measurements were performed using a resolution of 4 cm<sup>-1</sup> and 24 scans were accumulated for each sample. The micro-morphology of the microgel was analyzed using a Quanta 450 scanning electron microscope (FEI, USA). Nitrogen adsorption was performed using a JW-BK122W surface area and porosity analyzer (Gaobo, China). The surface area of the microgel

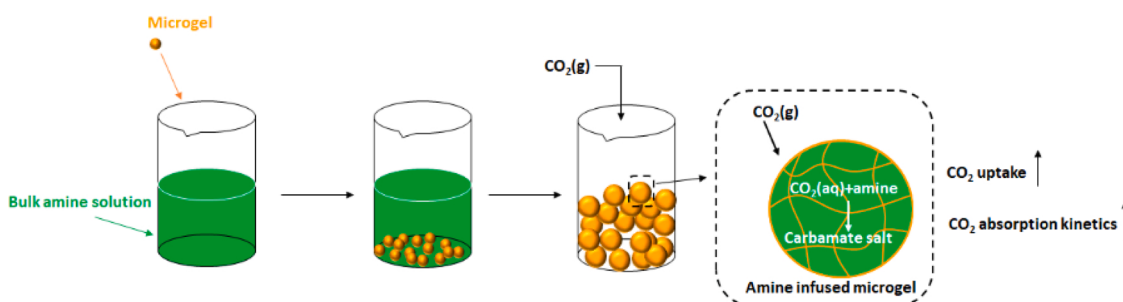


**Fig. 1.** Illustration of the enhancement effect of microgel on CO<sub>2</sub> capture capacity of amines.

was calculated from nitrogen adsorption data by Brunauer–Emmett–Teller (BET) analysis. An optical microscope (Leica, Germany) was used to observe the morphology of the AIMGs. The particle size distribution of the microgel was measured using a HYDRO2000 laser particle size analyzer (Malvern, UK). The thermogravimetric analysis of the microgel was studied using a thermogravimetric analyzer (NETZSCH, Germany). The test was carried out under nitrogen atmosphere at a constant flow rate of 60 mL/min and a heating rate of 10 °C/min with the temperature ranging from 40 to 800 °C.

#### 2.4. CO<sub>2</sub> absorption experiments

The experimental procedure is analogous to that proposed by (Dawson et al. (2014)) As shown in Fig. 2, typically, 1.0 g of amine aqueous solution with known concentration was loaded into a vial. Afterwards, 0.25 g of the microgel was added and blended with the amine solution. The mixture was then left for 5 min enabling the formation of the AIMG. The mass of the AIMG sample was measured and recorded. Since all the amine solution was absorbed by the microgel, the mass of the AIMG was approximately 1.25 g. Subsequently, the vial containing the AIMG sample was sealed by a screw cap with rubber septa and CO<sub>2</sub> gas was injected into the vial using a balloon equipped with a needle that penetrated the rubber septa. A second needle was also pierced the rubber septa as a vent thus enabling the CO<sub>2</sub> to flow freely in the vial. The CO<sub>2</sub> absorption lasted for 30 min. The mass of the AIMG increased during the CO<sub>2</sub> absorption and the increased mass was attributed to the absorbed CO<sub>2</sub>. The mass change of the AIMG sample during the CO<sub>2</sub> absorption was recorded and used for the calculation of the CO<sub>2</sub> uptake of the AIMG sample. All the experiments were performed under 25 °C. The temperature was precisely controlled by the water bath. The water attached on the external surface of the vial was dried before weighting the AIMG sample. For each scenario, three measurements were performed and the average value was taken as the CO<sub>2</sub> uptake. The experimental uncertainties were evaluated by the standard deviation and exhibited as error bars in the Fig. 5.

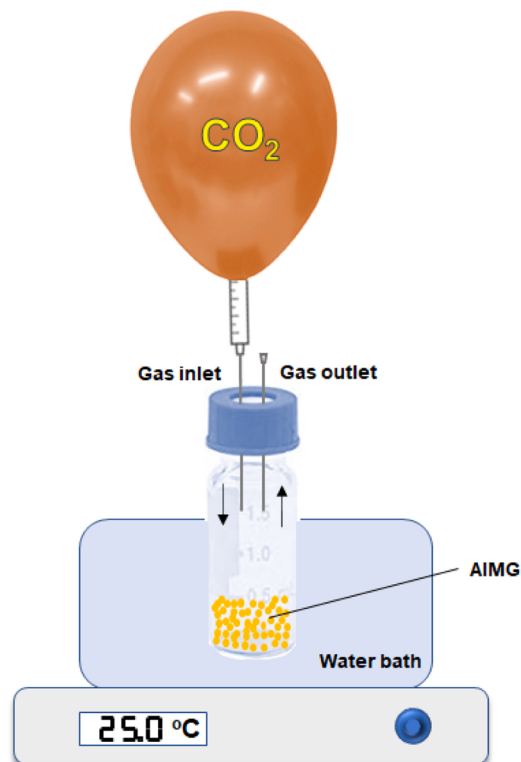


Fig. 2. Experimental schematic of the CO<sub>2</sub> absorption experiment.

#### 2.5. Regeneration performance

Temperature swing is a commonly used method for regeneration in CO<sub>2</sub> capture application. This method was also used in this study to evaluate the cyclic capability of AIMGs. In a typical cycle, a freshly prepared AIMG sample first underwent the CO<sub>2</sub> absorption experiments as stated above, then the CO<sub>2</sub>-loaded AIMG sample was placed in an oven for 30 min to desorb the loaded CO<sub>2</sub>. The temperature of the oven was demonstrated in Fig. 11. Distilled water was then added to the heated sample to make up for the evaporative solvent loss. The mass of the added distilled water was estimated by the mass difference of the freshly prepared sample (1.25 g) and the heated sample. Subsequently, the AIMG sample cooled down to ambient temperature before the next CO<sub>2</sub> absorption test was carried out. The CO<sub>2</sub> uptakes at multiple absorption–desorption cycles were recorded to assess the regeneration performance of the AIMGs.

### 3. Results and discussion

#### 3.1. Characterizations of the microgel and the AIMGs

Scanning electron microscopy (SEM) image of the microgel is shown in Fig. 3. The microgel exhibited spherical structure with a smooth surface. Furthermore, as shown in Figure S1, the particle size of the microgel was in the range of 0.4–91 μm with the median particle size of 13.04 μm. The micron scale size endowed the microgel with higher surface area compared to the millimeter scale hydrogel in our previous studies (Xu et al., 2018; Xu and Wood, 2018; Xu et al., 2019). The BET surface area of the microgel was 3.15 m<sup>2</sup>/g and the BET surface area of the hydrogel was 0.23 m<sup>2</sup>/g (Figure S2). The surface area of the microgel was approximately 13.7 times higher than the hydrogel. Figure S3 shows the FTIR spectrum of the microgel. The wide bands at 3334 cm<sup>-1</sup> and 3197 cm<sup>-1</sup> were attributed to the stretching vibration peaks of N—H. The absorption peak at 1655 cm<sup>-1</sup> was assigned to the stretching vibration of C=O. The absorption peak at 1547 cm<sup>-1</sup> was attributed to the bending vibration of N—H. The absorption peaks at 1188 cm<sup>-1</sup>, 1119 cm<sup>-1</sup> and 1041 cm<sup>-1</sup> were the characteristic peaks of the -SO<sub>3</sub><sup>-</sup> group. The thermal stability of the microgel (dry sample) was determined using thermal gravimetric (TG) analysis and the TG curve of the microgel is shown in Figure S4. The curve demonstrates three stages. The first stage occurred in the range of 40–287 °C with a mass loss of 13.03 wt%, which was ascribed to the evaporation of intramolecular and intermolecular moisture. The second stage occurred in the range of 287–563 °C with a

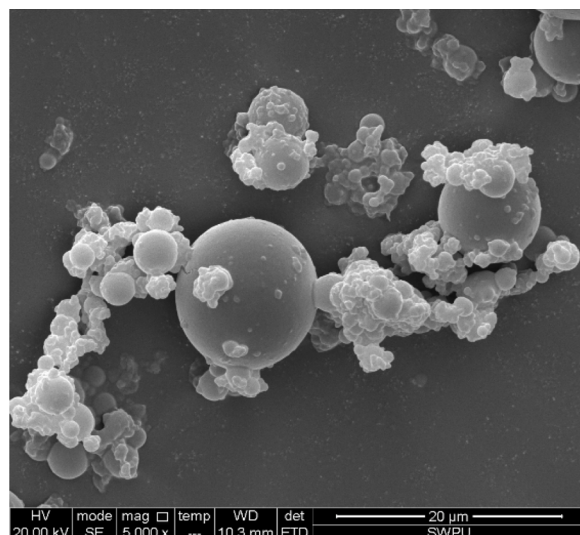
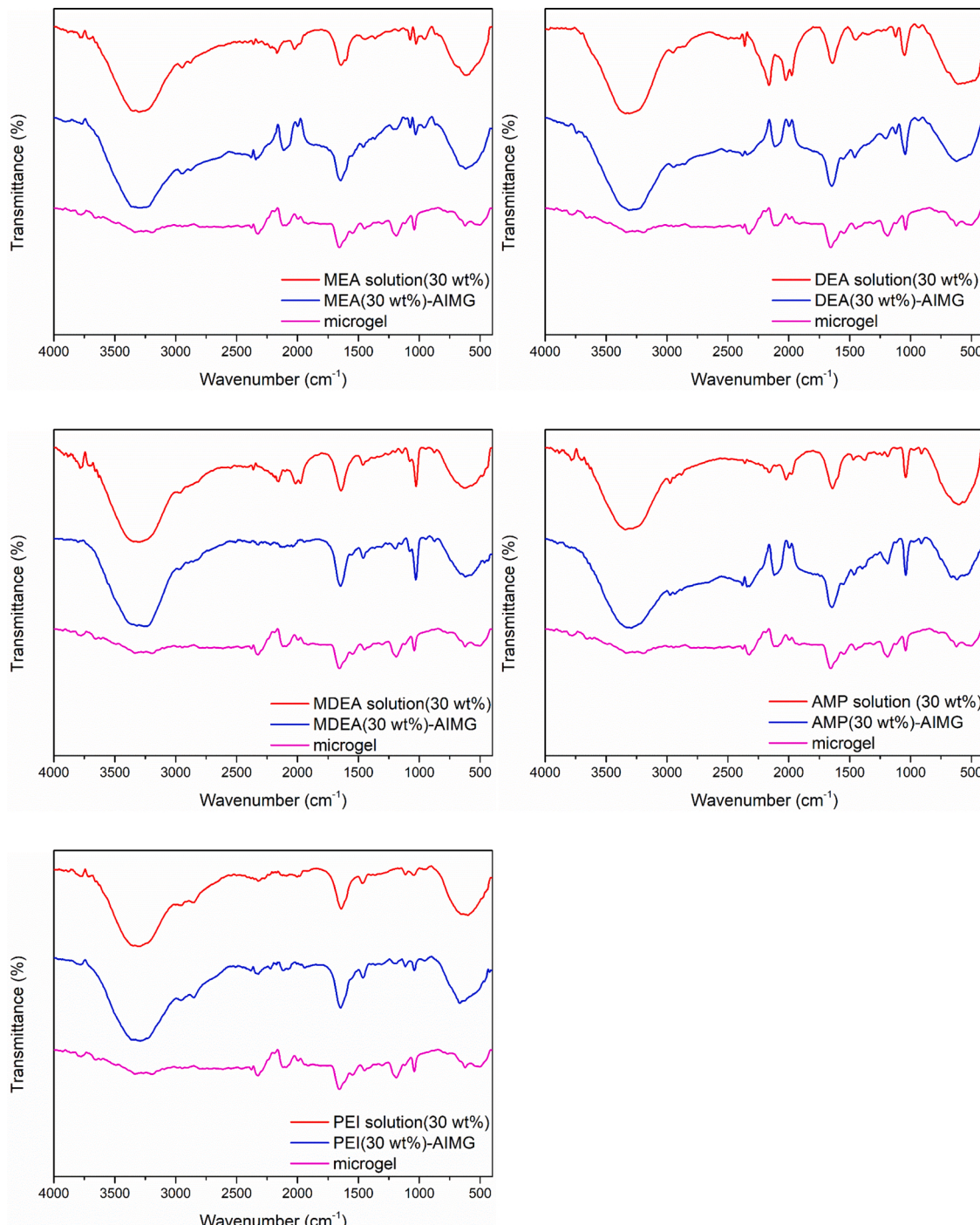


Fig. 3. SEM image of the microgel.

mass loss of 69.22 wt%, corresponding to the decomposition of amide groups and sulfonic acid groups. The final stage occurred beyond 563 °C with a mass loss of 8.18 wt%, which was attributed to the carbonization. According to the TG curve of the microgel, it can be found that the microgel was thermally stable up to at least 287 °C.

Five amine absorbents including MEA, DEA, MDEA, AMP, PEI were used to prepare different AIMGs. In each case, the amine concentration was fixed at 30 wt%. The microgel sample infused with deionized water was used in the tests for comparison. The optical microscope image of the AIMGs and the water infused microgel are shown in Figure S5. All the samples exhibited similar spherical structure. Furthermore, as shown in Fig. 4, compared to the FTIR spectrum of the microgel, there

are some new absorption peaks shown in the FTIR spectra of the AIMGs. It worth noting that these new absorption peaks can also be found in the FTIR spectra of the amine solutions. This indicates that the differences in the chemical structure between the microgel and the AIMGs were attributed to the introduction of amines. What's more, there was no additional peak appeared in the spectra of the AIMGs compare to that of the amine solutions and the microgel, demonstrating that there was no new material or group formed after infusing the amine solutions into the microgel. The microgel was mainly functioned as a support for the amine solutions, which transformed liquid amines into "solid state"



**Fig. 4.** FTIR spectra of the amine solutions, the AIMGs and the microgel.

### 3.2. $\text{CO}_2$ uptakes and $\text{CO}_2$ absorption kinetics of AIMGs

The  $\text{CO}_2$  uptakes and absorption kinetics of the AIMGs were studied over 30 min. To promote the  $\text{CO}_2$  solubility, the bulk amine solutions were stirred during the tests.

The  $\text{CO}_2$  uptake of the water infused microgel is shown in Fig. 5a. The  $\text{CO}_2$  uptake was only 1.2 mg/g absorbent when the absorption reached equilibrium. This demonstrates that the microgel itself has negligible capability in  $\text{CO}_2$  absorption.

As a primary amine, MEA is characterized through fast reaction kinetics and high  $\text{CO}_2$  absorbing capacity (Schaffer et al., 2012), making it one of most commonly used absorbent in the  $\text{CO}_2$  capture industry. As shown in Fig. 5b, the  $\text{CO}_2$  uptake of the stirred MEA solution reached 73.6 mg  $\text{CO}_2$ /g absorbent after absorbing  $\text{CO}_2$  for 30 min. According to the previous studies (Yang et al., 2015; Al-Azzawi et al., 2012), the formation of extremely viscous carbamate salts would substantially hamper the diffusion of the  $\text{CO}_2$  into amine solutions, which lowers the

$\text{CO}_2$  uptake of the amine solutions. Therefore, vigorous stirring increased the mass transfer between the gas-liquid interface and enhanced the  $\text{CO}_2$  uptake which, otherwise, would be lower. Nevertheless, despite the promotion resulting from the vigorous stirring, the  $\text{CO}_2$  uptake of the MEA solution was lower than the MEA-AIMG over the experimental timescale and 87.2 mg  $\text{CO}_2$ /g absorbent of  $\text{CO}_2$  uptake was achieved by the MEA-AIMG. Due to the negligible  $\text{CO}_2$  absorption capability of the microgel itself, the  $\text{CO}_2$  uptake of the MEA-AIMG was mainly attributed to the infused MEA. According to the MEA content and  $\text{CO}_2$  absorption amount, the MEA absorption efficiency was calculated. As shown in Table 1, the MEA absorption efficiency of MEA-AIMG was about 365.0 mg  $\text{CO}_2$ /g MEA and the MEA absorption efficiency of the MEA solution was only 245.3 mg  $\text{CO}_2$ /g MEA at the end of the experimental timescale. This demonstrates that the MEA absorption efficiency was enhanced by the formation of the MEA-AIMG. Compared to the MEA solution, the MEA-AIMG has different structure, different volume, and the same content of MEA. Therefore, the structure and volume have

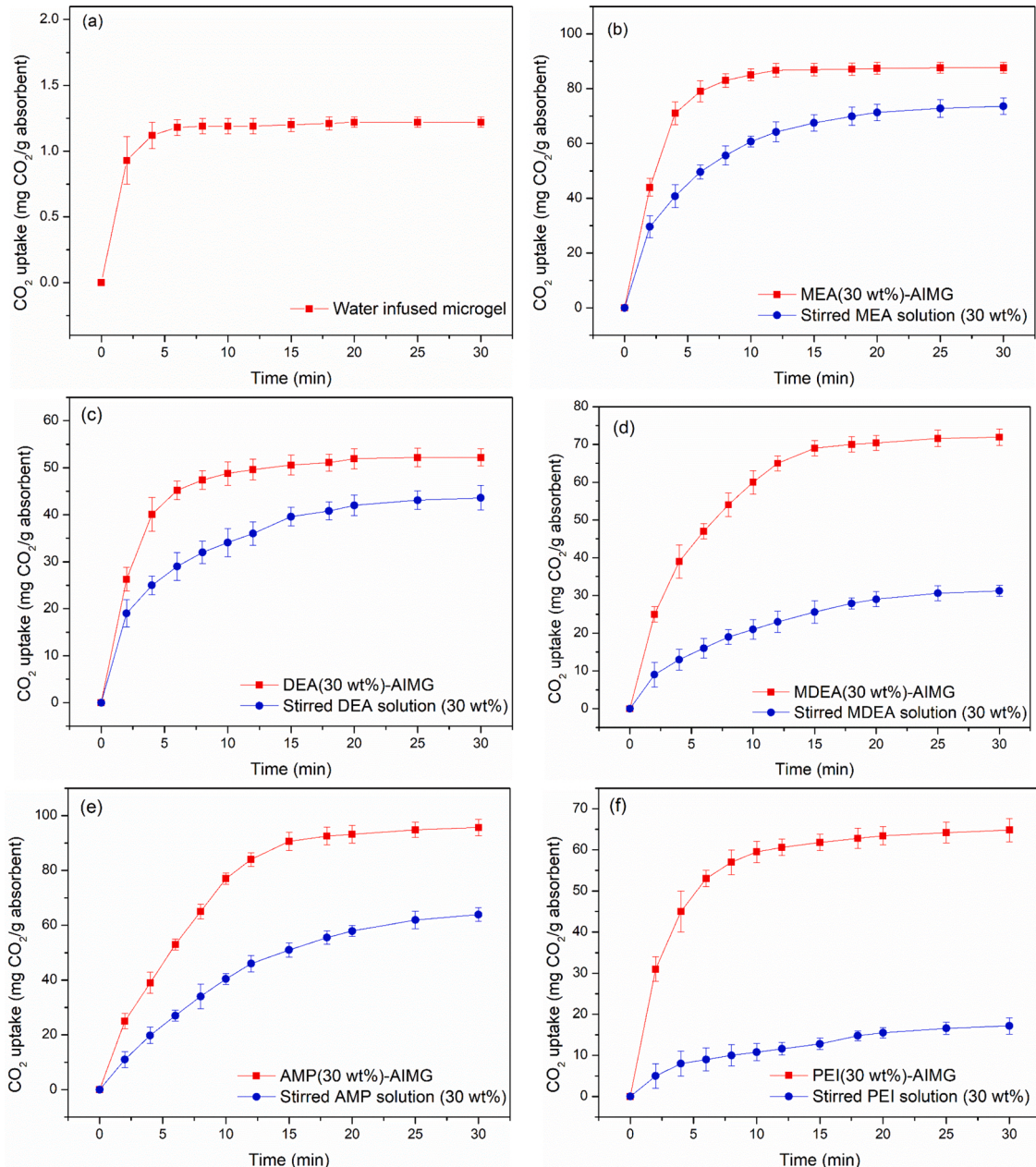


Fig. 5.  $\text{CO}_2$  uptake of various bulk amine solutions and AIMGs.

**Table 1**Summary of CO<sub>2</sub> absorption experiments.

Amine solution (30 wt%, g)	Microgel (g)	Stirring	95 % absorption time (min)	CO <sub>2</sub> absorption (mg)	Absorption efficiency* (mg of CO <sub>2</sub> /g of amine)
MEA	1.0	–	Yes	18.0	73.6
MEA	1.0	0.25	–	7.5	109.5
DEA	1.0	–	Yes	19.2	43.6
DEA	1.0	0.25	–	11.8	65.3
MDEA	1.0	–	Yes	24.6	31.2
MDEA	1.0	0.25	–	14.0	89.9
AMP	1.0	–	Yes	23.8	63.9
AMP	1.0	0.25	–	15.4	119.5
PEI	1.0	–	Yes	24.8	17.2
PEI	1.0	0.25	–	14.3	81.0

\* The absorption efficiency was calculated by the CO<sub>2</sub> absorption and the amine mass of the amine solutions and the AIMGs.

an effect on the enhancement of the MEA absorption efficiency and the effect would be discussed in Section 3.3 combined with the FTIR analysis. Additionally, the MEA-AIMG also exhibited faster absorption kinetics than the MEA solution. The time (*t*<sub>95</sub>) required to attain 95 % of the final CO<sub>2</sub> uptake of each experiment was used to characterize the absorption kinetics. The *t*<sub>95</sub> of the MEA-AIMG was roughly 58 % shorter than that of the MEA solution (Table 1).

As a secondary amine, DEA has a lower heat of reaction with CO<sub>2</sub> (76.3 kJ/mol CO<sub>2</sub>) compared to that of MEA (85.6 kJ/mol CO<sub>2</sub>) (Galindo et al., 2012). However, due to the relatively low CO<sub>2</sub> reactivity, DEA has a lower CO<sub>2</sub> absorption capacity than MEA. As shown in Fig. 5c, the CO<sub>2</sub> uptake of the stirred DEA solution was 43.6 mg CO<sub>2</sub>/g absorbent at the end of the experiment. In contrast, the DEA-AIMG exhibited 52.2 mg CO<sub>2</sub>/g absorbent of CO<sub>2</sub> uptake. Furthermore, as shown in Table 1, the absorption kinetics of the stirred DEA solution was slow and the *t*<sub>95</sub> of the DEA solution was 19.2 min, while the DEA-AIMG demonstrated much faster absorption kinetics and the *t*<sub>95</sub> was only 11.8 min. In addition, the absorption efficiency of DEA increased from 145.3–217.5 mg CO<sub>2</sub>/g DEA by forming the DEA-AIMG.

Compared to MEA and DEA, the tertiary alkanolamine MDEA possesses many advantages including better stability, lower corrosive, lower vapour pressure and lower absorption heats (Lu et al., 2005). Nevertheless, the relatively low reactivity and low CO<sub>2</sub> absorption rate of MDEA make it less competitive (Gabrielsen et al., 2007). As shown in Fig. 5d, the CO<sub>2</sub> uptake of the stirred bulk MDEA solution was only 31.2 mg CO<sub>2</sub>/g absorbent after CO<sub>2</sub> absorption for 30 min. The corresponding absorption efficiency of MDEA was 104 mg CO<sub>2</sub>/g MDEA (Table 1). To improve the absorption performance of MDEA, traditionally, activators such as MEA, DEA, and piperazine (PZ) (Appl et al., 1982; Chowdhury et al., 2013) were mixed with MDEA forming activated MDEA solutions. Recently, (Feng et al. (2013)) used an ionic liquid as an activator to enhance the CO<sub>2</sub> absorption capacity of MDEA. However, the activators are not necessary in terms of the MDEA-AIMG. The maximum CO<sub>2</sub> uptake of MDEA-AIMG in the experimental timescale was 71.9 mg CO<sub>2</sub>/g absorbent which is over 2 times higher than that of the stirred bulk MDEA solution. Meanwhile, the absorption efficiency of MDEA for the MDEA-AIMG was 299.7 mg CO<sub>2</sub>/g MDEA (Table 1). Additionally, the absorption kinetics of MDEA-AIMG was noticeably faster than that of the bulk MDEA, with the *t*<sub>95</sub> being approximately 49 % shorter.

AMP is a promising absorbent as a new class of CO<sub>2</sub> absorbents called sterically hindered amines (MacDowell et al., 2010). Despite the primary amine structure, the energy consumption of AMP during regeneration is lower than MEA due to the steric hindrance. In addition, unlike MEA or DEA which can only be loaded up to about 0.5 mol of CO<sub>2</sub>/mol of amine, AMP can reach loading of 1 mol of CO<sub>2</sub>/mol AMP (Khan et al., 2015). Therefore, the bulk AMP solution exhibited competitive CO<sub>2</sub> absorption capacity compared to other tested bulk amine solutions and 63.9 mg CO<sub>2</sub>/g absorbent of CO<sub>2</sub> uptake was achieved within 30 min (Fig. 5e). However, the absorption kinetics of the AMP solution was slow and the CO<sub>2</sub> uptake was unable to reach the plateau within the experimental timescale. In contrast, the AMP-AIMG

exhibited both superior CO<sub>2</sub> uptake and faster absorption kinetics. 95.6 mg CO<sub>2</sub>/g absorbent of CO<sub>2</sub> uptake was achieved by the AMP-AIMG and the *t*<sub>95</sub> of the AMP-AIMG was approximately 35 % shorter than that of the AMP solution (Table 1). The amine absorption efficiency of the AMP-AIMG (398.3 mg CO<sub>2</sub>/g AMP) was also significantly higher than that of the bulk AMP solution (213 mg CO<sub>2</sub>/g AMP), demonstrating effective enhancement in the CO<sub>2</sub> capture capacity of AMP.

PEI is one of the leading amines that are used for preparing solid CO<sub>2</sub> absorbents due to the low volatility and therefore favorable recyclability in temperature-swinging regeneration process. Furthermore, the high N/C ratio compared with other common amine absorbents means that PEI has superior CO<sub>2</sub> loading capacity and multiple nitrogen atoms in PEI macromolecular chain could serve as reactive centers for CO<sub>2</sub> absorbing. Nevertheless, the absorbent can be difficult to prepare and often suffers from low stability. In addition, the high viscosity of the PEI solution resulting from the macromolecular structure substantially hampers the diffusion of CO<sub>2</sub> molecules into the PEI solution. As a result, the CO<sub>2</sub> uptake of the PEI solution was only 17.2 mg CO<sub>2</sub>/g absorbent (Fig. 5f) and the absorption efficiency of PEI for the solution was only 57.3 mg CO<sub>2</sub>/g PEI (Table 1). The *t*<sub>95</sub> of the PEI solution was approximately 24.8 min. In contrast, the PEI-AIMG exhibited much better CO<sub>2</sub> absorption capacity and faster absorption kinetics, with 64.8 mg CO<sub>2</sub>/g absorbent of CO<sub>2</sub> uptake and 270 mg CO<sub>2</sub>/g PEI of PEI absorption efficiency were achieved in the experimental timescale and the *t*<sub>95</sub> of the PEI-AIMG was approximately 14.3 min.

### 3.3. FTIR analysis

Infrared spectroscopy measurements were carried out in order to study the mechanism of CO<sub>2</sub> binding of the AIMGs. According to the FTIR spectra of the water infused microgel (Fig. 6), there was no new absorption peak appeared after CO<sub>2</sub> absorption, demonstrating that the chemical groups of the microgel would not react with CO<sub>2</sub>. Therefore, the CO<sub>2</sub> uptake of the water infused microgel could be attributed to dissolution of CO<sub>2</sub> in the water existing in the microgel. In contrast, the FTIR spectra of all the AIMGs exhibited new absorption peaks after CO<sub>2</sub> absorption. It worth noting that these new peaks could also be found in the FTIR spectra of the amine solutions after absorption. Therefore, these new peaks could be attributed to the formation of carbamate and bicarbonate. For example, the new absorption peaks at 1531 cm<sup>-1</sup>, 1413 cm<sup>-1</sup>, 1361 cm<sup>-1</sup>, and 1300 cm<sup>-1</sup> appeared in the FTIR spectrum of the DEA-AIMG after CO<sub>2</sub> absorption. In the FTIR spectrum of the DEA solution, the new peaks appeared in the same wavenumbers after CO<sub>2</sub> absorption. The absorption peaks at 1531 cm<sup>-1</sup> and 1413 cm<sup>-1</sup> were attributed to the stretching vibration of the COO- and the C—N, respectively (Galperin and Finkelshtein, 1972; Frasco, 1964). The absorption peaks at 1361 cm<sup>-1</sup> and 1300 cm<sup>-1</sup> were assigned to the stretching vibration of —CO— and bending vibration of —COH of the HCO—<sub>3</sub><sup>-</sup> (Milella and Mazzotti, 2019; Davis and Oliver, 1972). By contrast, due to the different amine structure, there was only bicarbonate formed after CO<sub>2</sub> absorption for the MDEA-AIMG.

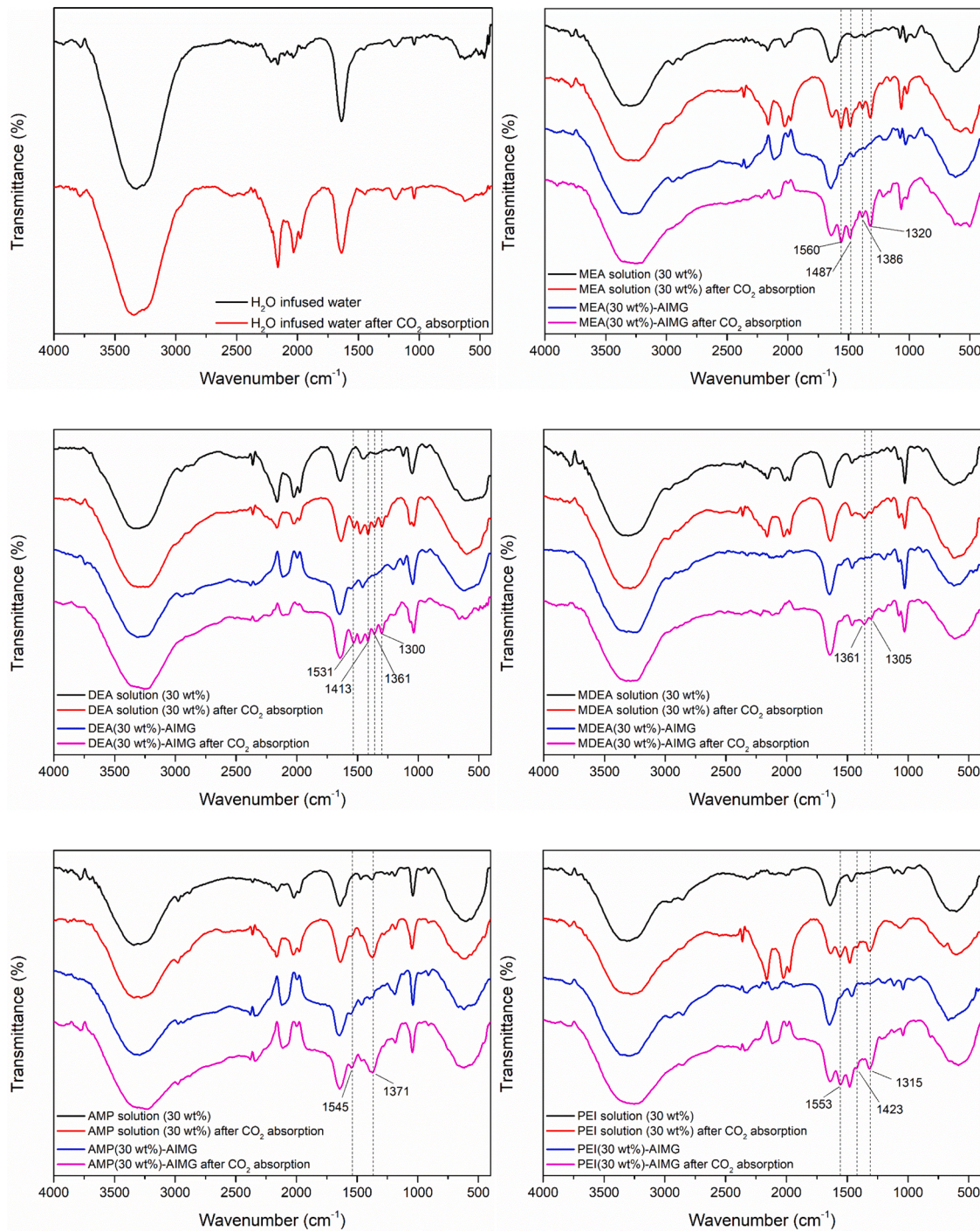


**Fig. 6.** FTIR spectra of the amine solutions and the AIMGs before and after  $\text{CO}_2$  absorption.

Correspondingly, the characterization peak of the  $\text{COO}^-$  was not observed in the FTIR spectrum of the MDEA-AIMG. The characterization peaks of the  $\text{HCO}_3^-$  at  $1361\text{ cm}^{-1}$  and  $1305\text{ cm}^{-1}$  appeared in the FTIR spectrum of the MDEA-AIMG after  $\text{CO}_2$  absorption. Similarly, the characterization peaks of the  $\text{COO}^-$  or/and the  $\text{HCO}_3^-$  can also be found in the FTIR spectra of other samples. The detailed assignment of these peaks is included in Table S1. In brief, according to the FTIR analysis, it can be found that the  $\text{CO}_2$  absorption mechanism of the AIMGs is the same as that of the amines. The  $\text{CO}_2$  loading capacity and reactivity are quite different for MEA, DEA, MDEA, AMP, and PEI. Accordingly, the  $\text{CO}_2$  uptake and absorption kinetics were different for the different AIMGs which was mentioned in Section 3.2.

Despite the same  $\text{CO}_2$  absorption mechanism and the same amine content, the AIMGs exhibited higher  $\text{CO}_2$  uptake and faster absorption kinetics than the corresponding amine solutions. This could be attributed to the different structure and volume of the two systems. Compared to the amine solutions, the addition of the microgel increased the volume of the AIMGs and transformed the bulk solution into separated “solid” particles. It has been reported that molecules and ions significantly smaller than the size of the polymer network in hydrogels are capable of diffusing into hydrogels as fast as in water (Yue et al., 2014; Nayak and Lyon, 2005). Therefore, the diffusion rate of the small  $\text{CO}_2$  molecule into the bulk solution and the microgel was similar. However, as shown in Fig. 7, the space among the AIMG particles provided

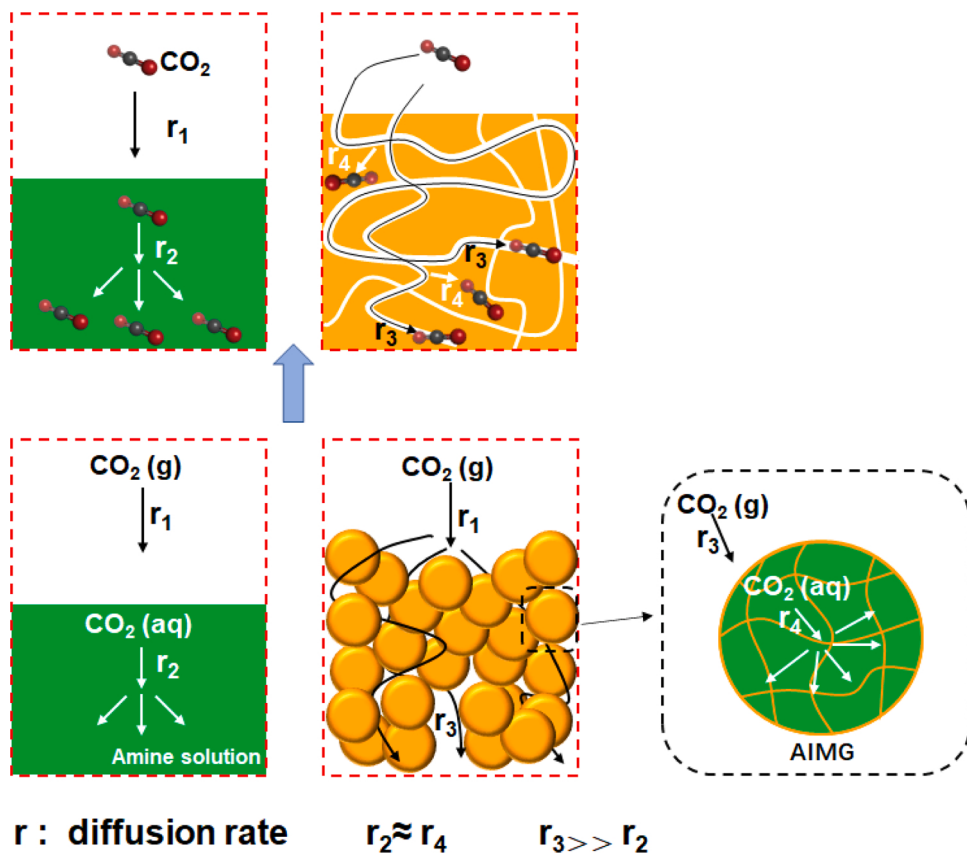


Fig. 7. Schematic diagram of  $\text{CO}_2$  diffusion in the amine solutions and the AIMGs.

diffusion channels for the  $\text{CO}_2$  molecule and the diffusion rate of the  $\text{CO}_2$  molecule in the space was much faster than that into the bulk solution. If the separated AIMG particles were treated as a bulk, the "AIMG bulk" was filled with many high-speed diffusion channels for the  $\text{CO}_2$  molecule. This would effectively increase the contact efficiency of the amines and the  $\text{CO}_2$ . Therefore, the AIMGs exhibited superior  $\text{CO}_2$  capture performance compared to the amine solutions.

In our previous studies (Xu and Wood, 2018), the amine infused hydrogels (AIHs) also exhibited superior  $\text{CO}_2$  capture performance than the amine solutions. The data of the AIHs is also listed in Table S1 for comparison. Despite the different chemical structure of the AIMGs and the AIHs, the  $\text{CO}_2$  binding mechanism of the two systems are similar, which is attributed to the infused amines. Therefore, the difference in the  $\text{CO}_2$  capture performance for the two systems was mainly resulted from the morphology. The relatively smaller size of the AIMGs endowed the system with higher BET surface area which is more than 10 times than that of the AIHs. As a result, the AIMGs exhibited much faster absorption kinetics compared to the AIHs. The  $t_{95\%}$  of all the AIMGs were significantly lower than that of the corresponding AIHs. The higher surface area of the AIMGs provided more contact area for  $\text{CO}_2$  and amines, which accelerates the reaction rate. However, the higher surface area did not lead to higher amine absorption efficiency. The amine absorption efficiency of amines of the AIMGs and AIHs was quite close. This may be because the diffusion capability of the  $\text{CO}_2$  molecule into the microgel or the hydrogel was related to the concentration of carbamate or bicarbonate. The extremely viscous carbamate or bicarbonate would substantially hamper the diffusion of the  $\text{CO}_2$  molecule. It is possible that the  $\text{CO}_2$  molecule was unable to diffuse into the microgel or the hydrogel when the concentration of carbamate or bicarbonate reached a certain value and the value was related to the chemical structure of amines. Therefore, the  $\text{CO}_2$  absorption efficiency of the AIMG and AIH was similar for the same amine solution.

### 3.4. Optimization of the AIMGs

As mentioned in the above section, all AIMGs displayed higher  $\text{CO}_2$  uptakes and faster absorption kinetics than the corresponding bulk amine solutions, demonstrating a wide applicability to various amine species. Nevertheless, in terms of the application in industrial  $\text{CO}_2$  capture projects, the AIMGs need to be further optimized to achieve the best performance.

In a typical amine scrubbing process, the commonly used amine concentration is approximately 30 wt% because higher amine concentrations would result in excessive corrosion and foaming issue (Rochelle, 2009; Dawson et al., 2014). However, when it comes to AIMGs, the amine solutions are 'locked' in solid microgel particles and therefore the foaming issue could be avoided. Furthermore, the AIMGs were much less corrosive than their bulk solution counterparts. For example, as shown in Fig. 8, the color of pH indicator paper immediately changed after contacting with the MEA solution (30 wt%). In contrast, the change of the pH paper was negligible when the pH paper was contacted with the MEA-IMG. The microgel particles significantly minimized the direct contact between MEA and the pH paper by 'locking' the MEA solution inside the network structure, which contributes to mitigating the corrosion of amines to equipment in terms of industry application. This would require further corrosion testing but this is a good indication. Therefore, it is feasible to use more concentrated amine solutions in the formation of AIMGs.

In order to determine the optimum concentration, the effect of amine concentration on the  $\text{CO}_2$  absorbing capacity of AIMGs was comprehensively studied. Amine solutions with various concentrations were used to prepare AIMGs. Typically, the AIMGs were comprised of 1.0 g of amine solutions and 0.25 g of microgel particles. The formation time was set as 5 min. As shown in Fig. 9, the  $\text{CO}_2$  uptakes of the AIMGs increased with the increase in amine concentration at first and then decreased.

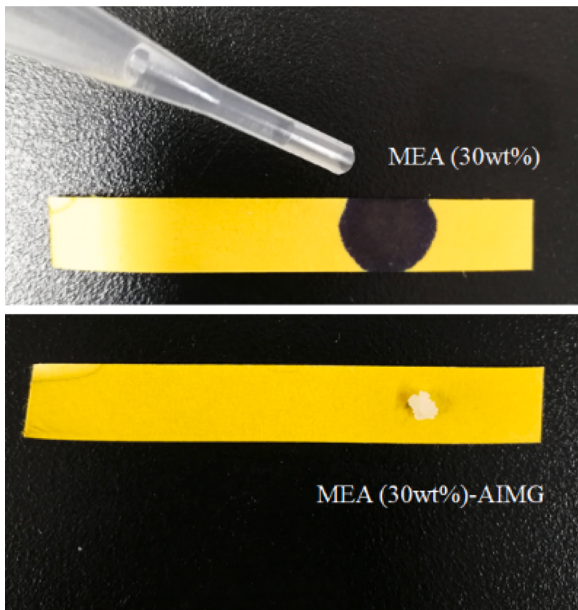


**Fig. 8.** pH measurements of the MEA solution and the MEA-AIMG.

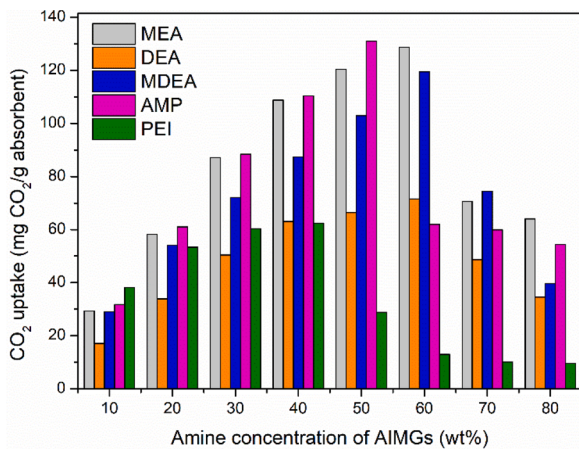


**Fig. 9.** CO<sub>2</sub> uptake of AIMGs with different amine concentrations.

When the amine concentration was 10 wt%, PEI-AIMG exhibited the highest CO<sub>2</sub> uptake among all the AIMGs, which may result from the relatively high N/C ratio of PEI compared with other amines. However, the viscous carbamate salts formed by PEI and

CO<sub>2</sub> became more pronounced with the increase in PEI concentration. When the amine concentration increased to 40 wt%, the CO<sub>2</sub> uptakes of other AIMGs surpassed that of PEI-AIMG and PEI-AIMG exhibited the lowest CO<sub>2</sub> uptake among all the AIMGs. With the amine concentration further increased from 40 wt% to 80 wt%, the CO<sub>2</sub> uptakes of all the AIMGs reached peaks and then decreased. This is because the microgel was unable to absorb the whole amine solution within the formation time (5 min) when the amine concentration was above a certain value. For example, as shown in Fig. 10, the DEA-AIMG was well-formed when the DEA concentration increased from 10 wt% to 60 wt%, while excessive DEA solution was observed when the DEA concentration reached 70 wt%. As a result, the CO<sub>2</sub> uptake of DEA-AIMG substantially decreased when the DEA concentration increased from 60 wt% to 70 wt %. When the DEA concentration was increased to 80 wt%, the DEA-AIMG was not even formed and the microgel particles were soaked in the excessive DEA solution demonstrating a form of suspension. Therefore, the CO<sub>2</sub> uptake of the DEA-AIMG was even lower when the

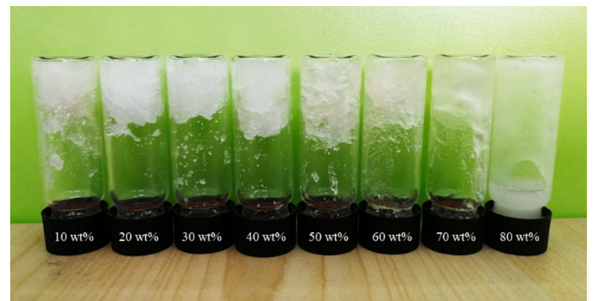


**Fig. 10.** DEA-AIMG prepared with the microgel and DEA solution with different concentrations within 5 min.

DEA concentration increased to 80 wt%. Likewise, the MEA-AIMG, MDEA-AIMG, AMP-AIMG and PEI-AIMG exhibited the peak CO<sub>2</sub> uptakes when the amine concentrations were 60 wt%, 60 wt%, 50 wt% and 40 wt%, respectively. The optimum amine concentrations for different AIMGs were different, which is attributed to the varied swelling capability of the microgel in different amine solutions. Normally, the swelling ratio of hydrogel relates closely to the solution properties such as salinity, polarity, and pH (Bajpai and Giri, 2003; Huang et al., 2007). Due to the different chemical structures of MEA, DEA, MDEA, AMP and PEI, the polarities of the amine solutions were different. Therefore, the microgels exhibited different swelling capability. Furthermore, it is worth noting that the optimum amine concentrations are likely to be enhanced if a higher microgel addition was used in the preparation of the AIMGs but this would increase the cost of AIMGs. In addition, a longer formation time for AIMGs could also enhance the optimum amine concentrations. For example, the DEA-AIMG with 70 wt% of DEA was formed when the formation time extended from 5 min to 30 min. However, the longer formation time might be an issue in industrial application because the productivity would be reduced. Therefore, considering the above reasons, 60 wt% MEA, 60 wt% DEA, 60 wt% MDEA, 50 wt% AMP and 40 wt% PEI were selected as the optimum amine concentrations for the AIMGs in this study. These AIMGs with the optimum amine concentrations are referred to as MEA(60 wt%)-AIMG, DEA(60 wt%)-AIMG, MDEA(60 wt%)-AIMG, AMP(50 wt%)-AIMG, and PEI(40 wt%)-AIMG, respectively.

### 3.5. Regeneration performance of AIMGs

A vital property for maintaining CO<sub>2</sub> capture efficiency of absorbents is the stability under regeneration. Therefore, multiple cycles of CO<sub>2</sub> absorption and desorption were carried out to study the regeneration performance of the AIMGs with the optimum amine concentrations. As shown in Fig. 11, the CO<sub>2</sub> uptake of the MEA(60 wt%)-AIMG dropped by 89.8 % after ten cycles. Considering that the network structure of the microgel was thermally stable up to at least 287 °C which has been proved by TG, the loss in CO<sub>2</sub> uptake is mainly associated with the high volatility of MEA. By contrast, the DEA(60 wt%)-AIMG, the MDEA(60 wt %)-AIMG and the AMP(50 wt%)-AIMG exhibited better regeneration performance owing to the lower volatility of the amines. The CO<sub>2</sub> uptakes of the DEA(60 wt%)-AIMG, the MDEA(60 wt%)-AIMG and the AMP(50 wt%)-AIMG decreased by 29.7 %, 12.9 % and 15.7 %, respectively, after ten cycles. Unsurprisingly, due to the extremely low volatility of PEI, the PEI(40 wt%)-AIMG displayed the most encouraging regeneration performance over ten absorption-desorption cycles, with the CO<sub>2</sub> uptake only decreasing by 3.2 %. However, the high regeneration temperature of the PEI(40 wt%)-AIMG may pose high energy consumption for the regeneration process. The heat consumption of the AIMGs remains to be shown in further studies. In terms of industrial application, the volatility of amines in the AIMGs should be seriously considered. Therefore, an appropriate equipment should be designed and installed on the top of absorbers if the AIMGs were used for carbon

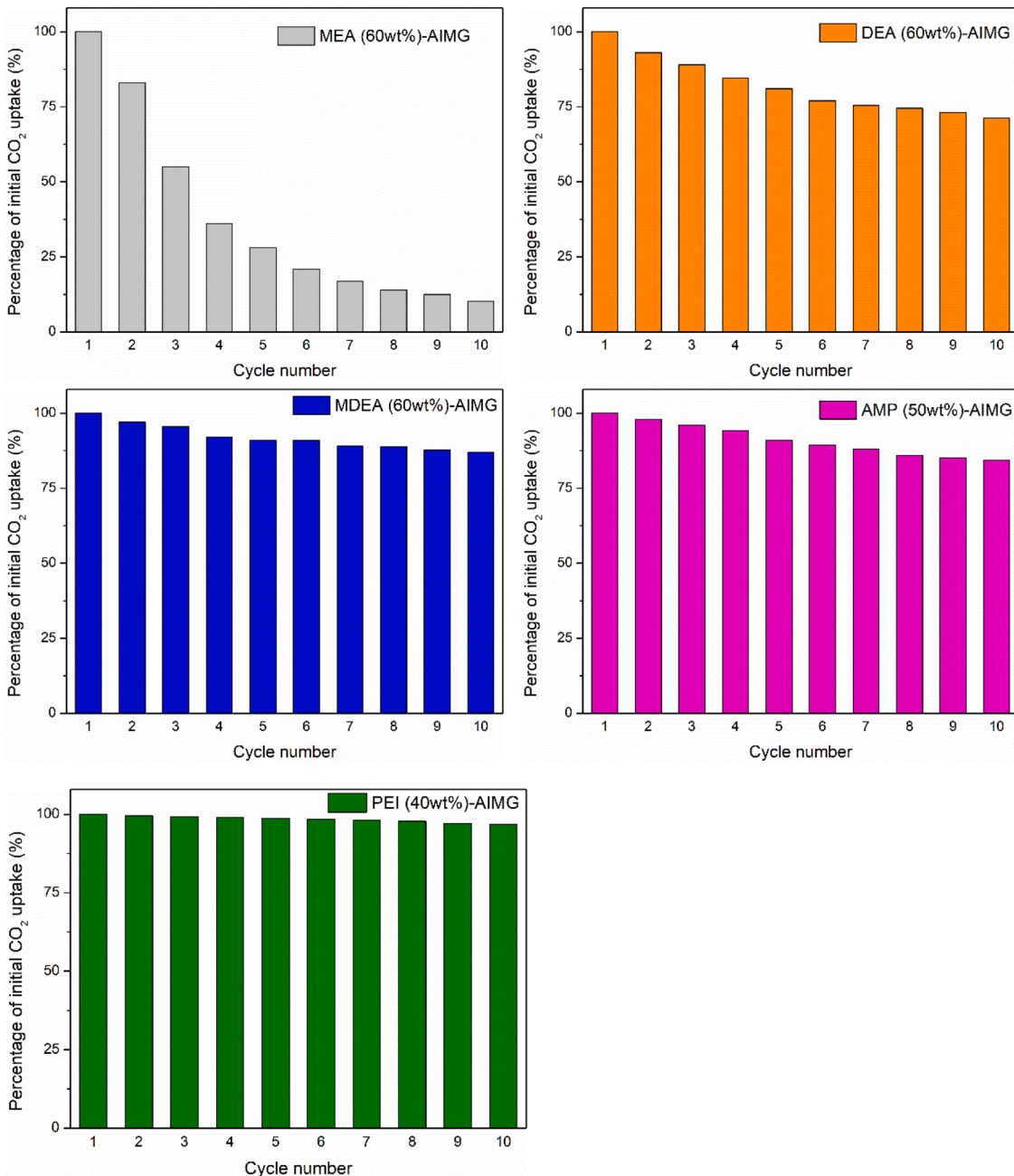


**Fig. 11.** Regeneration performance of AIMGs. (Regeneration temperatures of the MEA-AIMG, DEA-AIMG, MDEA-AIMG, AMP-AIMG, and PEI-AIMG were 95 °C, 85 °C, 80 °C, 80 °C and 160 °C, respectively.).

capture in industrial scale, which would be considered in the future studies.

#### 4. Conclusions

In this study, a microgel prepared through inversion emulsion polymerization was used to demonstrate the concept of the study. The proposed amine infused microgels (AIMGs) are promising candidates for CO<sub>2</sub> capture. By using microgel particles as micro-reactors, the AIMGs demonstrated several advantages over the conventional bulk amine solutions. First of all, due to the solid particle structure, the space among the AIMG particles provided diffusion channels for the CO<sub>2</sub> molecule and enhanced the contact efficiency of the amines and CO<sub>2</sub>. As a result, the AIMGs exhibit higher CO<sub>2</sub> uptake and faster absorption kinetics than the conventional amine solutions. Furthermore, ‘locking’ the amine

solutions in the microgel particles contributes to mitigating the corrosion and foaming issues of the amine solutions. Therefore, the amine solutions which have higher concentrations than the commercial counterparts were able to be used in the preparation of AIMGs, which further enhances the CO<sub>2</sub> capture capacity of AIMGs. In addition, owing to the thermally stable network structure, the AIMGs which were prepared by the amines with low volatility exhibited favorable cyclic capacity during the temperature-swing regeneration process. For large-scale application, the CO<sub>2</sub> capture capacity of the AIMGs under high temperature and high pressure and the long-term stability of the AIMGs need to be considered. Nevertheless, the proof-of-concept study has demonstrated that infusing amine solutions into microgel particles forming AIMGs is a feasible and facile approach to enhance the CO<sub>2</sub> capture capacity of amine solutions.

## Author statements

- Yang Yang: conceptualization and experimental measurements
- Xingguang Xu: formal analysis of results, methodology, writing and reviewing
- Yunfei Guo: formal analysis of results, writing and reviewing, and funding acquisition
- Colin D. Wood: conceptualization and formal analysis of results

## Declaration of Competing Interest

The authors confirm that there are no conflicts of interest to report.

## Acknowledgements

Financial support for this work by the Chengdu University of Technology and CSIRO is gratefully acknowledged.

## Appendix A. Supplementary data

Supplementary material related to this article can be found, in the online version, at doi:<https://doi.org/10.1016/j.ijggc.2020.103172>.

## References

- Al-Azzawi, O.M., Hofmann, C.M., Baker, G.A., Baker, S.N.J., 2012. Nanosilica-supported polyethoxamines as low-cost, reversible carbon dioxide sorbents. *J. Colloid Interface Sci.* 385, 154–159.
- Bajpai, A.K., Giri, A., 2003. Water sorption behaviour of highly swelling (carboxy methylcellulose-g-polyacrylamide) hydrogels and release of potassium nitrate as agrochemical. *Carbohyd. polym.* 53 (3), 271–279.
- Chowdhury, F.A., Yamada, H., Higashii, T., Goto, K., Masami, O., 2013. CO<sub>2</sub> capture by tertiary amine absorbents: a performance comparison study. *Ind. Eng. Chem. Res.* 52, 8323–8331.
- Davis, A.R., Oliver, B.G., 1972. A vibrational-spectroscopic study of the species present in the CO<sub>2</sub>-H<sub>2</sub>O system. *J. Solution Chem.* 1 (4), 329–339.
- Dawson, R., Cooper, A.I., Adams, D.J., 2013. Chemical functionalization strategies for carbon dioxide capture in microporous organic polymers. *Polym. Int.* 62, 345–352.
- Dawson, R., Stevens, L.A., Williams, O.S.A., Wang, W., Carter, B.O., Sutton, S., Drage, T.C., Blanc, F., Adams, D.J., Cooper, A.I., 2014. Impact of Water Coadsorption for Carbon Dioxide Capture in Microporous Polymer Sorbents. *Energy Environ. Sci.* 7, 1786–1791.
- Feng, Z., Gao, Y., Wu, X., Ma, J., Wu, Y., Zhang, Z., 2013. Regeneration performance of amino acid ionic liquid (AAIL) activated MDEA solutions for CO<sub>2</sub> capture. *Chem. Eng. J.* 223, 371–378.
- Fine, N.A., Goldman, M.J., Rochelle, G.T., 2014. Nitrosamine formation in amine scrubbing at desorber temperatures. *Environ. Sci. Technol.* 48 (15), 8777–8783.
- Frasco, D.L., 1964. Infrared spectra of ammonium carbamate and deutoeroammonium carbamate. *J. Chem. Phys.* 41, 2134–2140.
- Gabrielsen, J., Svendsen, H.F., Michelsen, M.L., Stenby, E.H., Kontogeorgis, G.M., 2007. Experimental validation of a rate-based model for CO<sub>2</sub> capture using an AMP solution. *Chem. Eng. Sci.* 62 (9), 2397–2413.
- Galindo, P., Schaffer, A., Brechtel, K., Unterberger, S., Scheffknecht, G., 2012. Experimental research on the performance of CO<sub>2</sub>-loaded solutions of MEA and DEA at regeneration conditions. *Fuel* 101, 2–8.
- Galperin, V.A., Finkelstein, A.I., 1972. Infrared spectra of ammonium carbamate and bicarbonate. *J. Appl. Spectrosc.* 17, 1176–1178.
- Goeppert, A., Meth, S., Prakash, G.K.S., Olah, G.A., 2010. Nanostructured silica as a support for regenerable high-capacity organoamine-based CO<sub>2</sub> sorbents. *Energy Environ. Sci.* 3 (12), 1949–1960.
- Huang, Y., Yu, H., Xiao, C., 2007. pH-sensitive cationic guar gum/poly (acrylic acid) polyelectrolyte hydrogels: swelling and in vitro drug release. *Carbohyd. Polym.* 69 (4), 774–783.
- Khan, A.A., Halder, G.N., Saha, A.K., 2015. Carbon dioxide capture characteristics from flue gas using aqueous 2-amino-2-methyl-1-propanol (AMP) and monoethanolamine (MEA) solutions in packed bed absorption and regeneration columns. *Int. J. Greenh. Gas Con.* 32, 15–23.
- Lu, Y., Proch, S., Schrinner, M., Kempe, R., Ballauff, M., 2009. Thermosensitive core-shell microgel as a "nanoreactor" for catalytic active metal nanoparticles. *J. Mater. Chem.* 19 (23), 3955–3961.
- Lu, J., Wang, L., Sun, X., Li, J., Liu, X., 2005. Absorption of CO<sub>2</sub> into aqueous solutions of methylidethanolamine and activated methylidethanolamine from a gas mixture in a hollow fiber contactor. *Ind. Eng. Chem. Res.* 44 (24), 9230–9238.
- Luo, Q., Liu, P., Guan, Y., Zhang, Y., 2010. Thermally Induced Phase Transition of Glucose-Sensitive Core-Shell Microgels. *ACS Appl. Mater. Interfaces* 2, 760–767.
- MacDowell, N., Florin, N., Buchard, A., Hallett, J., Galindo, A., Jackson, G., Adjiman, C. S., Williams, C.K., Shah, N., Fennell, P., 2010. An overview of CO<sub>2</sub> capture technologies. *Energy Environ. Sci.* 3, 1645–1669.
- Milella, F., Mazzotti, M., 2019. Estimating speciation of aqueous ammonia solutions of ammonium bicarbonate: application of least squares methods to infrared spectra. *React. Chem. Eng.* 4, 1284–1302.
- Nayak, S., Lyon, L.A., 2005. Soft nanotechnology with soft nanoparticles. *Angew. Chem. Int. Edit.* 44 (47), 7686–7708.
- Nur, H., Snowden, M.J., Cornelius, V.J., Mitchell, J.C., Harvey, P.J., Benée, L.S., 2009. Colloidal microgel in removal of water from biodiesel. *Colloids Surf., A* 335, 133–137.
- Oh, J.K., Drumright, R., Siegwart, D.J., Matyjaszewski, K., 2008. The development of microgels/nanogels for drug delivery applications. *Prog. Polym. Sci.* 33 (4), 448–477.
- Pu, W., Zhao, S., Wang, S., Wei, B., Yang, C., Li, Y., 2018. Investigation into the migration of polymer microspheres (PMs) in porous media: implications for profile control and oil displacement. *Colloids Surf. A* 540, 265–275.
- Raynal, L., Bouillon, P.A., Gomez, A., Broutin, P., 2011. From MEA to demixing solvents and future steps, a roadmap for lowering the cost of post-combustion carbon capture. *Chem. Eng. J.* 171 (3), 742–752.
- Rochelle, G.T., 2009. Amine scrubbing for CO<sub>2</sub> capture. *Science* 325 (5948), 1652–1654.
- Romeo, L.M., Bolea, I., Escosa, J.M., 2008. Integration of power plant and amine scrubbing to reduce CO<sub>2</sub> capture costs. *Appl. Therm. Eng.* 28 (8), 1039–1046.
- Samanta, A., Zhao, A., Shimizu, G.K.H., Sarkar, P., Gupta, R., 2011. Post-combustion CO<sub>2</sub> capture using solid sorbents: a review. *Ind. Eng. Chem. Res.* 51, 1438–1463.
- Schaffer, A., Brechtel, K., Scheffknecht, G., 2012. Comparative study on differently concentrated aqueous solutions of MEA and TETA for CO<sub>2</sub> capture from flue gases. *Fuel* 101, 148–153.
- Schmidt, S., Motschmann, H., Hellweg, T., Klitzing, R.V., 2008. Thermoresponsive surfaces by spin-coating of PNIPAM-co-PAA microgels: A combined AFM and ellipsometry study. *Polymer* 49 (3), 749–756.
- Soosaiprakasam, I.R., Veawab, A., 2008. Corrosion and polarization behavior of carbon steel in MEA-based CO<sub>2</sub> capture process. *Int. J. Greenh. Gas Con.* 2 (4), 553–562.
- Stuckert, N.R., Yang, R.T., 2011. CO<sub>2</sub> capture from the atmosphere and simultaneous concentration using zeolites and amine-grafted SBA-15. *Environ. Sci. Technol.* 45, 10257–10264.
- Sumida, K., Rogow, D.L., Mason, J.A., McDonald, T.M., Bloch, E.D., Herm, Z.R., Bae, T., Long, J.R., 2011. Carbon dioxide capture in metal-organic frameworks. *Chem. Rev.* 112 (2), 724–781.
- Wiese, S., Spiess, A.C., Richtering, W., 2013. Microgel-Stabilized Smart Emulsions for Biocatalysis. *Angew. Chem. Int. Ed.* 125 (2), 604–607.
- Woodward, R.T., Stevens, L.A., Dawson, R., Vijayaraghavan, M., Hasell, T., Silverwood, I.P., Ewing, A.V., Ratvijitvech, T., Exley, J.D., Chong, S.Y., Blanc, F., Adams, D.J., Kazarian, S.G., Snape, C.E., Drage, T.C., Cooper, A.I., 2014. Swellable, Water- and Acid-Tolerant Polymer Sponges for Chemoselective Carbon Dioxide Capture. *J. Am. Chem. Soc.* 136 (25), 9028–9035.
- Wulff, G., Chong, B.O., Kolb, U., 2006. Soluble Single-Molecule Nanogels of Controlled Structure as a Matrix for Efficient Artificial Enzymes. *Angew. Chem., Int. Ed.* 45, 2955–2958.
- Xu, X., Wood, C.D., 2018. A highly tunable approach to enhance CO<sub>2</sub> capture with liquid Alkali/amines. *Environ. Sci. Technol.* 52 (18), 10874–10882.
- Xu, X., Heath, C., Pejicic, B., Wood, C.D., 2018. CO<sub>2</sub> capture by amine infused hydrogels (AIHs). *J. Mater. Chem. A* 6 (11), 4829–4838.
- Xu, X., Yang, Y., Acenosio Falcon, L.P., Hazewinkel, P., Wood, C.D., 2019. Carbon capture by DEA-infused hydrogels. *Int. J. Greenh. Gas Con.* 88, 226–232.
- Yang, J., Yu, X., Yan, J., Tu, S., 2014. CO<sub>2</sub> capture using amine solution mixed with ionic liquid. *Ind. Eng. Chem. Res.* 53 (7), 2790–2799.
- Yang, J., Han, H.Y., Low, Q.X., Binks, B.P., Chin, J.M., 2015. CO<sub>2</sub> capture by dry alkanolamines and an efficient microwave regeneration process. *J. Mater. Chem. A* 3, 6440–6446.
- Yao, D., Li, T., Zheng, Y., Zhang, Z., 2019. Fabrication of a functional microgel-based hybrid nanofluid and its application in CO<sub>2</sub> gas adsorption. *React. Funct. Polym.* 136, 131–137.
- Yue, M., Hoshino, Y., Ohshiro, Y., Imamura, K., Miura, Y., 2014. Temperature-Responsive Microgel Films as Reversible Carbon Dioxide Absorbents in Wet Environment. *Angew. Chem. Int. Ed.* 53, 2692–2695.
- Zhu, D., Hou, J., Chen, Y., Zhao, S., Bai, B., 2018. In situ surface decorated polymer microsphere technology for enhanced oil recovery in high-temperature petroleum reservoirs. *Energy Fuels* 32 (3), 3312–3321.
- Appl, M.; Wagner, U.; Henrici, H. J.; Kuessner, K.; Voldamer, K.; Fuerest, E. Removal of CO<sub>2</sub> and/or H<sub>2</sub>S and/or COS from Gas Containing These Constituents. U.S. Patent 4,336,233, 1982.